European Journal of Medicinal Chemistry 46 (2011) 2609–2616

Contents lists available at ScienceDirect

European Journal of Medicinal Chemistry

journal homepage: http://www.elsevier.com/locate/ejmech

Original article

Synthesis and evaluation of heterobivalent tacrine derivatives as potential multi-functional anti-Alzheimer agents

Wen Luo, Yan-Ping Li, Yan He, Shi-Liang Huang, Ding Li, Lian-Quan Gu, Zhi-Shu Huang*

School of Pharmaceutical Sciences, Sun Yat-sen University, Guangzhou 510006, People's Republic of China

ARTICLE INFO

Article history:
Received 12 December 2010
Received in revised form
26 February 2011
Accepted 25 March 2011
Available online 3 April 2011

Keywords:
Tacrine
Alzheimer's disease
Cholinesterase
Antioxidant
β-Amyloid

ABSTRACT

A new series of heterobivalent tacrine derivatives were designed, synthesized and evaluated as potential multi-functional anti-Alzheimer agents for their inhibitory activity on cholinesterases, antioxidant activity and self-induced β-amyloid (Aβ) aggregation. All these synthesized compounds had potent inhibition activity on acetylcholinesterase (AChE) and butyrylcholinesterase (BuChE) at nanomolar range. A Lineweaver–Burk plot and molecular modeling study showed that these compounds targeted both the catalytic active site (CAS) and the peripheral anionic site (PAS) of AChE. The compounds containing hydroxyl group showed potent peroxyl radical absorbance activity. In addition, compound **5j** exhibited higher self-induced Aβ aggregation inhibitory activity than curcumin, which could become a multi-functional agent for further development for the treatment of AD.

1. Introduction

Alzheimer's disease (AD) is a progressive neurodegenerative brain disorder that is characterized by dementia, cognitive impairment, and memory loss [1]. It affects millions of elder peoples, and the number of patients is expected to increase in the next 20 years. Many factors have been found to be implicated in AD, and its etiology and pathogenesis remain unclear. There are diverse hallmarks such as low levels of acetylcholine, oxidative damage and β-amyloid (Aβ) deposits, which seem to play significant roles in the disease [2]. Current treatment of AD focuses on increasing cholinergic neurotransmission in the brain by inhibiting cholinesterases (ChEs) with medicines including donepezil, rivastigmine and galantamine (Fig. 1) [3]. But clinical experience shows that inhibition of ChEs is a palliative treatment, which does not address AD's etiology [4]. Due to the multi-pathogenesis of AD, one of the current strategies is to develop novel anti-AD agents with multiple potencies [5].

In recent years, more and more attention is paid to oxidative stress for its role in the progression of AD [6]. An increasing research has suggested that oxidative stress is involved in the early stage of the pathogenesis and plays an important factor to initiate the aggregation of Aβ and τ-protein hyperphosphorylation. Many evidences support that antioxidants could be able to attenuate the syndrome of AD, and prevent the progression of the disease [7]. Thus, drugs that specifically scavenge oxygen radicals could be useful for either the prevention or the treatment of AD [8].

The progressive deposition of Aβ is generally considered to be fundamental to the development of neurodegenerative pathology [9]. There are two principal forms of Aβ, and Aβ42 and Aβ40 are the main components of the plaques in the brain tissue of AD patients [10]. However, compared to relatively soluble Aβ40, Aβ42 is more prone to aggregation and more neurotoxic. Therefore, the prevention of Aβ42 formation or aggregation is currently another potential method for treatment of AD [11,12], and some related inhibitors including curcumin [13,14] and benzofuran analogs [15,16] have been developed.

Tacrine (Fig. 1) is the first approved ChEs inhibitor by the FDA for the treatment of AD. This medicine has some side effects, therefore, the search for tacrine derivatives is still of interest. In recent years, many studies have focused on the combined effects of ChEs inhibition and scavenging oxygen radicals as well as reduction of the Aβ fibril self-aggregation by conjugating tacrine with other active groups. Based on this strategy, many tacrine derivatives [17–20] (A–D in Fig. 1) have been designed and synthesized.

Our research group has been involved in the development of potential drugs for the treatment of AD for many years [21–23]. In the present study, we are interested in the development of tacrine derivatives as multi-functional agents that could possibly bind with

* Corresponding author. Tel.: +8620 39949056; fax: +8620 39943056.
E-mail address: ceshzs@mail.sysu.edu.cn (Z.-S. Huang).

0223-5234/$ – see front matter © 2011 Elsevier Masson SAS. All rights reserved.
doi:10.1016/j.ejmech.2011.03.058

both the peripheral and catalytic site of acetylcholinesterase, and also have antioxidation or anti-Aβ aggregation activity. The tacrine derivatives were designed because of the following reasons. Firstly, tacrine is a well-known ChEs inhibitor for the treatment of AD. Next, it has been reported that compounds containing electron-rich aromatic groups could possibly bind to the peripheral binding site of acetylcholinesterase (E in Fig. 1) [24]. Besides, docking studies have indicated that hydroxyl group on the benzene ring could form hydrogen bonds with residues in the binding site of ChE [25]. In addition, curcumin has a hydroxyl group on its benzene ring, which has potent antioxidation activity. Other compounds with similar structures might also have antioxidation activity. Here we report our results on the synthesis and biological evaluation of a series of new tacrine derivatives combined with aromatic groups as potential multi-functional agents for the treatment of AD.

2. Chemistry

Tacrine derivatives **5a**–**5r** were prepared with a sequence of reactions as shown in Scheme 1. Compounds **5c**–**5f** and **5p** were reported in our previous work [26]. In our preliminary results [26] and many other reports [17,27] on bivalent inhibitors connecting 1,2,3,4-tetrahydroacridine moieties with an alkyl linker, a heptylene or octylene has been found to be the optimal spacer, therefore, compounds **5i**–**5p** with octylene linker with various substituted aromatic groups were designed. It has been well-known that compounds containing pyridine group such as nicotine exhibited anti-Aβ aggregation and activity of scavenging free radicals [28,29], therefore, compounds **5q** and **5r** were also synthesized.

Intermediate compound **3** was synthesized from anthranilic acid in 90% overall yield with a previously reported procedure [30]. Then, reaction of compound **3** with alkylamine under reflux for 18 h in 1-pentanol gave 9-alkylamino-tetra-hydroacridines **4a**–**4e** in good yields (60–70%). In our experiment, this step was modified and carried out in the presence of catalytic amount of KI, and the reaction time was shortened obviously with slightly increased reaction yield. In the next step, the target compounds **5a**–**5q** were obtained by the reaction of aldehyde with intermediate **4** followed with reduction using $NaBH_4$ in methanol [31]. Compound **5r** was prepared in a solution of pyridine-4-carboxylic acid, *N*,*N*′-diisopropylcarbodiimide (DIC) and 4-dimethylaminopyridine (DMAP) in dichloromethane at room temperature (Scheme 1).

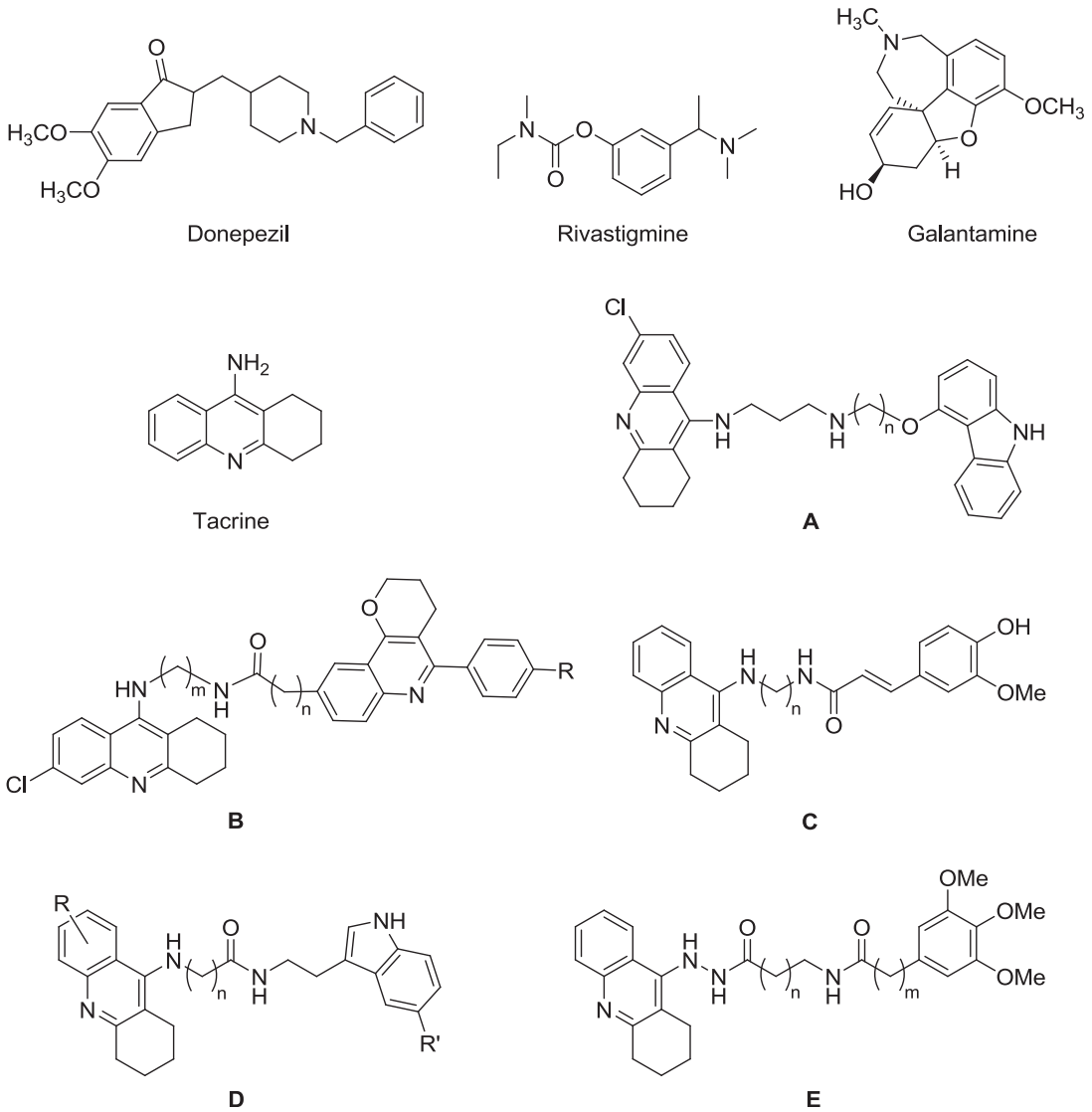

Fig. 1. Chemical structures of donepezil, rivastigmine, galantamine, tacrine, and tacrine derivatives.

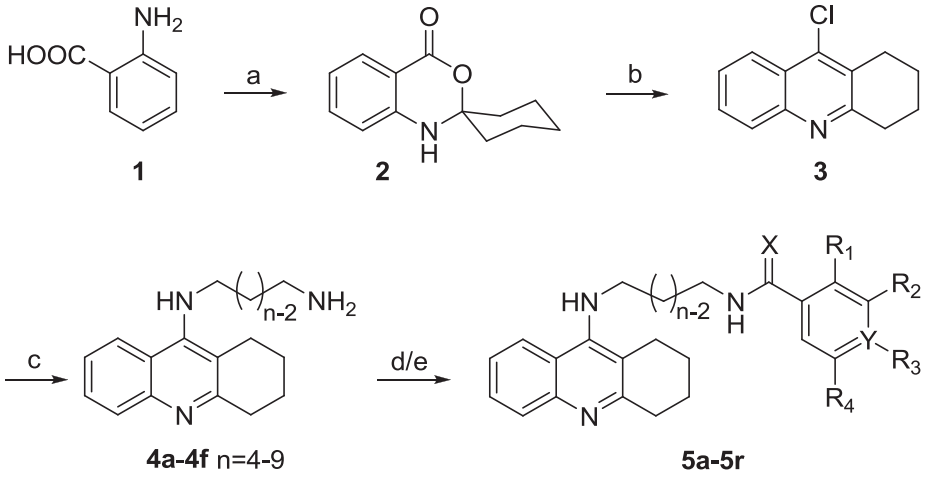

Scheme 1. Synthetic pathways for tacrine derivatives **5a**–**5r**. Reagents and conditions: (a) cyclohexanone, toluene, reflux; (b) $POCl_3$, 120 °C; (c) diamine, KI, 1-pentanol, 160 °C; (d) for **5a**–**5q**: 1. ArCHO, methanol, rt, 2. $NaBH_4$, methanol, rt, (e) for **5r**: pyridine-4-carboxylic acid, DIC, DMAP, CH_2Cl_2, rt.

3. Results and discussion

3.1. Inhibition studies on AChE and BuChE

The inhibitory activity of our synthetic derivatives was evaluated against AChE and BuChE with tacrine as a positive control using the method of Ellman et al. [32]. The IC_{50} values and selectivity index for the inhibition of AChE and BuChE were summarized as shown in Table 1 (data of **5c**–**5f** and **5p** were taken from ref [26]). Generally, most of these synthetic compounds showed good inhibition selectivity for BuChE over AChE. Recently BuChE has been considered as a potential drug target because it also regulates acetylcholine levels, and concurrent inhibition of both ChEs has been shown to provide additional benefits in the treatment of Alzheimer's disease [24].

Comparing compounds with the same dimethoxy group in aromatic ring (**5a**–**5f**), compound **5e** with a 8-methylene linker showed the best inhibition for AChE. The inhibition activity of

Table 1
Inhibition of ChEs by target compounds, and their selectivity index and oxygen radical absorbance capacity (ORAC).

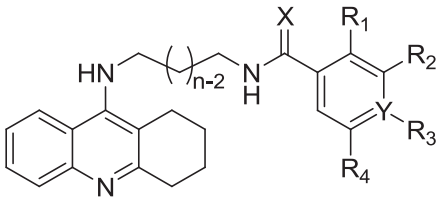

Compd	n	X	Y	R group	IC_{50}[a] for AChE (nM)	IC_{50}[b] for BuChE (nM)	Selectivity index[c]	Trolox [equiv][d]
5a	4	H_2	C	$R_1 = R_4 = H$, $R_2 = R_3 = OMe$	365.2 ± 7.8	37.2 ± 0.6	9.8	0.20 ± 0.02
5b	5	H_2	C	$R_1 = R_4 = H$, $R_2 = R_3 = OMe$	104.4 ± 0.2	24.4 ± 0.8	4.3	0.31 ± 0.03
5c[e]	6	H_2	C	$R_1 = R_4 = H$, $R_2 = R_3 = OMe$	30.9 ± 2.7	2.68 ± 0.17	11.5	0.42 ± 0.01
5d[e]	7	H_2	C	$R_1 = R_4 = H$, $R_2 = R_3 = OMe$	24.0 ± 0.3	5.51 ± 0.10	4.4	0.13 ± 0.02
5e[e]	8	H_2	C	$R_1 = R_4 = H$, $R_2 = R_3 = OMe$	11.35 ± 0.19	5.57 ± 0.83	2.0	0.11 ± 0.01
5f[e]	9	H_2	C	$R_1 = R_4 = H$, $R_2 = R_3 = OMe$	25.1 ± 3.0	5.67 ± 0.32	4.4	0.22 ± 0.03
5g	6	H_2	C	$R_1 = R_2 = R_4 = H$, $R_3 = OH$	25.6 ± 0.9	7.50 ± 0.02	3.4	2.7 ± 0.2
5h	6	H_2	C	$R_1 = R_4 = H$, $R_2 = OMe$ $R_3 = OH$	43.6 ± 1.2	9.28 ± 0.24	4.7	2.5 ± 0.2
5i	8	H_2	C	$R_1 = R_2 = R_4 = H$, $R_3 = OH$	7.48 ± 0.39	5.31 ± 0.13	1.4	2.6 ± 0.2
5j	8	H_2	C	$R_1 = R_4 = H$, $R_2 = OMe$, $R_3 = OH$	4.55 ± 0.13	3.41 ± 0.17	1.3	1.9 ± 0.1
5k	8	H_2	C	$R_1 = H$, $R_2 = R_4 = OMe$, $R_3 = OH$	4.61 ± 0.21	4.08 ± 0.24	1.1	1.2 ± 0.1
5l	8	H_2	C	$R_1 = R_3 = R_4 = H$, $R_2 = OH$	15.1 ± 0.2	4.91 ± 0.30	3.1	2.1 ± 0.1
5m	8	H_2	C	$R_1 = OH$, $R_2 = R_3 = R_4 = H$	12.5 ± 0.4	10.2 ± 0.3	1.2	2.4 ± 0.1
5n	8	H_2	C	$R_1 = R_2 = R_4 = H$, $R_3 = OMe$	15.3 ± 0.2	4.82 ± 0.41	3.2	0.32 ± 0.02
5o	8	H_2	C	$R_1 = R_4 = H$, R_2+$R_3 = OCH_2O$	6.14 ± 1.04	3.44 ± 0.02	1.8	0.12 ± 0.01
5p[e]	8	H_2	C	$R_1 = H$, R_2+$R_3 = OCH_2O$, $R_4 = OMe$	7.98 ± 0.12	7.94 ± 0.02	1.0	0.21 ± 0.03
5q	8	H_2	N	–	4.70 ± 0.30	4.66 ± 0.44	1.0	0.32 ± 0.03
5r	8	O	N	–	38.5 ± 2.4	38.7 ± 2.7	1.0	0.42 ± 0.01
Tacrine	–	–	–	–	193 ± 2	27.1 ± 1.2	7.1	<0.01

[a] AChE from *electric eel*; IC_{50}, inhibitor concentration (means ± SEM of three experiments) for 50% inhibition of AChE.
[b] BuChE from *equine serum*; IC_{50}, inhibitor concentration (means ± SEM of three experiments) for 50% inhibition of BuChE.
[c] Selectivity Index = IC_{50} (AChE)/IC_{50} (BuChE).
[d] Data are expressed as (μmol trolox)/(μmol tested compound).
[e] Data of ChEs inhibition were taken from ref [26].

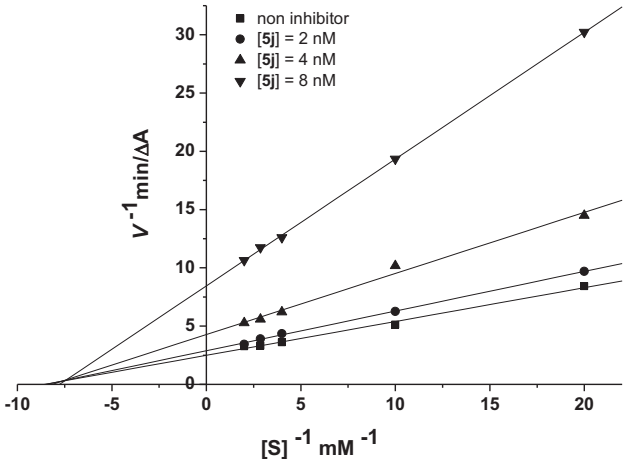

Fig. 2. Lineweaver–Burk plot for the inhibition of acetylcholinesterase by compound **5j**.

compounds **5i** and **5j** for AChE was better than that of compounds **5g** and **5h**. Their inhibitory activity for BuChE was not significantly affected by their chain length, which may be due to the conformational flexibility of the enzyme, as reported previously [3,22].

With the same chain length (**5i**–**5p**), all of these compounds exhibited more potent inhibition activity on both AChE and BuChE than tacrine. Their IC_{50} values for AChE were less than 16 nM, and their IC_{50} values for BuChE were less than 10 nM. Compound **5j** was found to have the best inhibitor for both ChEs with its IC_{50} values of 4.55 nM and 3.41 nM respectively, while the IC_{50} values of compounds **5i** and **5k** were very close to those of compound **5j**. It seems that the hydroxyl group at the 4′ position of the benzene ring was beneficial for their activity. This was in agreement with our results from molecular modeling studies, which indicated that this hydroxyl group formed hydrogen bond with the residue in the binding site of ChEs.

Compound **5q** containing a pyridine group with a 8-methylene linker also showed very potent activity for both ChEs. The methylene on the pyridine of compound **5q** was replaced with an amide group in compound **5r**, and the resulting inhibition activity of compound **5r** for both ChEs was decreased for 10 times lower than that of compound **5q**.

3.2. Kinetic studies for the inhibition of AChE

The nature of AChE inhibition by the best inhibitor compound **5j** was studied through the graphical analysis of steady state inhibition data, as shown in Fig. 2 [23]. The Lineweaver–Burk plots showed both increasing slopes and increasing intercepts at higher inhibitor concentration. This pattern indicated a mixed-type inhibition, which was similar to that of tacrine. This result showed that compound **5j** could bind to both CAS and PAS of AChE, which was consistent with the results of molecular modeling studies.

3.3. Studies of antioxidation activity

The peroxyl radicals reduced by the target compounds were determined by using the ORAC (oxygen radical absorbance capacity) assay [19], and the result was shown in Table 1. The activity of the compounds to scavenge radicals was expressed as Trolox equivalent, and their relative activity at concentrations between 1 and 5 μM was compared with that of the highly potent compound Trolox. Our result indicated that tacrine exhibited insignificant radical-capture capacity, while the compounds containing hydroxyl group showed potent peroxyl radical absorbance capacities ranging from 1.2- to 2.7-fold of the trolox value. After connecting the hydroxyl moiety to the tacrine, the resulting compounds showed obvious antioxidation activity. However, compounds **5q** and **5r** containing pyridine group showed relatively lower activity.

3.4. Molecular modeling

In order to understand the binding interactions between our synthetic compounds and *Tc*AChE (PDB code: 1ACJ), molecular modeling study was carried out using docking program AUTODOCK

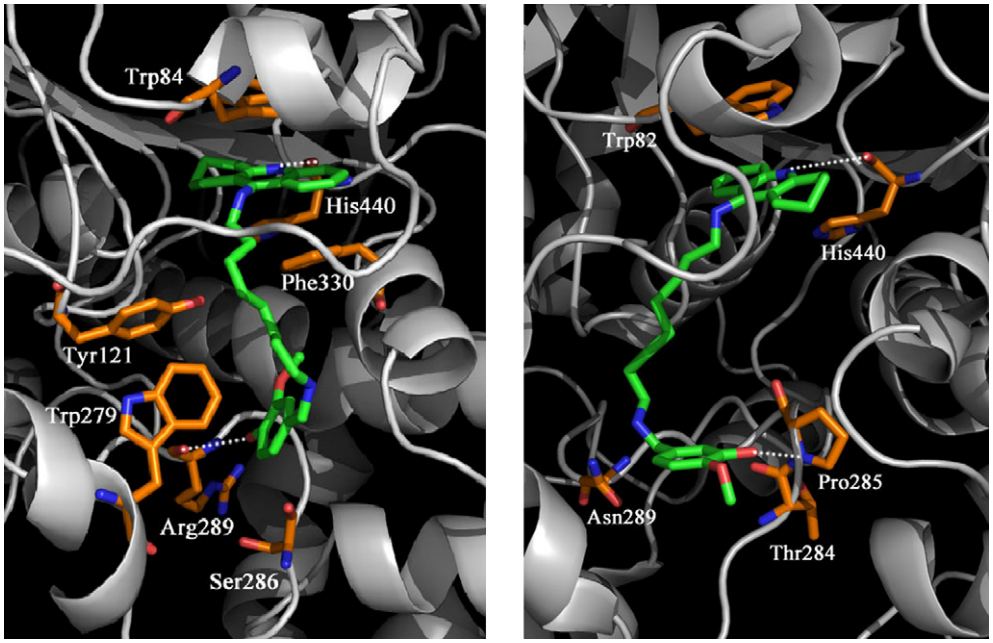

Fig. 3. Docking models of enzyme–compound complex. Compound **5j** interacts with residues in the binding site of *Tc*AChE and *Hu*BuChE. The compounds are rendered in green stick models, and the residues are rendered in orange sticks. Pictures were generated with PyMOL. (For interpretation of the references to colour in this figure legend, the reader is referred to the web version of this article.)

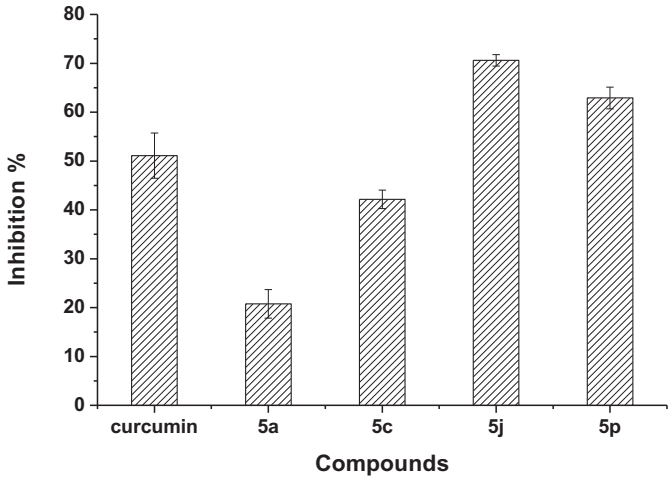

Fig. 4. Inhibition of self-mediated Aβ(1–42) aggregation by compounds **5a**, **5c**, **5j**, and **5p** comparing with that of curcumin. The measurements were carried out in the presence of 20 μM compounds. The mean ± SD values from three independent experiments were shown. Data of **5p** were taken from ref [26].

4.0 package with PyMOL program [33,34], and the result is shown in Fig. 3. Our docking studies indicated that all of these compounds exhibited multiple binding modes with AChE. In the complex of *Tc*AChE-**5j**, compound **5j** occupied the entire enzymatic CAS, mid-gorge and PAS. The tacrine moiety was bound to CAS with a classic π–π stacking interaction between Trp84 and Phe330. Their ring-to-ring distance was between 3.4 Å and 3.8 Å, and the protonated nitrogen atom of the quinoline ring had a hydrogen bond (3.4 Å) interaction with the carbonyl group of His440. In the PAS, a hydrogen bond was observed between the hydroxyl group and Arg289 with a distance of 3.3 Å. These results may explain why compound **5j** had potent inhibition for AChE. The docking studies showed that our compounds had a mixed type of inhibition, which was consistent with our kinetic analysis result. Because the crystal structure of BuChE from equine serum had not been reported, and the sequences of BuChE from equine showed high homology with that of human BuChE, so, the crystal structure of HuBuChE was used in the docking study. The similar interactions were also observed in the complex of *Hu*BuChE-**5j** (enzyme PDB code: 1POI). A π–π stacking interaction was found between tacrine and Trp82, and a hydrogen bond was observed between the hydroxyl group and Pro285 with a distance of 3.4 Å.

3.5. Inhibition of self-mediated Aβ(1–42) aggregation

We further evaluated the activity of some selected compounds to inhibit the self-mediated Aβ (1–42) aggregation using thioflavin T (ThT) assay [35]. Compared with the reference compound curcumin, the results showed that compounds **5j** apparently prevented the self-mediated Aβ aggregation with inhibition ratio of 71% (Fig. 4), which were higher than that of curcumin (50%). The activity of compounds **5a** and **5c** was lower than that of curcumin. The most potent compound was **5j**. It has been hypothesized that organic compounds with antioxidation activity could bind specifically to Aβ or Aβ fibril, but the mechanisms remain unknown [36].

4. Conclusion

In summary, thirteen new heterobivalent tacrine derivatives (**5a**, **5b**, **5g**–**5o**, **5q**, **5r**) were synthesized and characterized. Our results showed that these synthetic compounds had high ChEs inhibitory potency and good selectivity for BuChE over AChE. Compound **5j** exhibited the highest inhibitory effect for both ChEs. The inhibition kinetic analysis and molecular modeling study indicated that compound **5j** had binding with both CAS and PAS of the AChE. Besides, the compounds containing hydroxyl substitutive group had significant peroxyl radical absorbance capacity. In addition, compound **5j** exhibited higher self-induced Aβ aggregation inhibitory activity than curcumin. Our present results indicate that this new type of multi-functional compounds may provide a useful template for the development of new anti-AD agents with multiple potencies.

5. Experimental section

5.1. Chemistry

^{1}H and ^{13}C NMR spectra were recorded using TMS (tetramethyl silicane) as the internal standard in $CDCl_3$ with a Bruker BioSpin GmbH spectrometer at 400 MHz and 100 MHz, respectively. High resolution mass spectra (HRMS) were recorded on Shimadzu LCMS-IT-TOF. Flash column chromatography was performed with silica gel (200–300 mesh) purchased from Qingdao Haiyang Chemical Co. Ltd. The purities of synthesized compounds were confirmed to be higher than 95% by using analytical HPLC with a dual pump Shimadzu LC-20AB system equipped with an Ultimate XB-C18 column (4.6 × 250 mm, 5 μm) and eluted with methanol/water (35:65 to 45:55) containing 0.1% TFA (trifluoroacetic acid) at a flow rate of 0.5 mL/min.

5.1.1. Synthesis of intermediate 4

Intermediate **4** was prepared according to the previous literature procedure in our lab [26].

5.1.2. General procedures for the preparation of compounds ***5a***–***5q***

Aromatic aldehydes (1 mmol) and intermediate **4** (1 mmol) were stirred in MeOH for 4 h, and then were reduced through reaction with $NaBH_4$ (4 mmol) at room temperature for 4 h. The solvent was evaporated, and the residue was poured into water and extracted with ethyl acetate. The combined organic layers were dried over $MgSO_4$ and then concentrated. The resulting crude product was purified by flash chromatography with chloroform/methanol/ammonia as elution solvent. **5c**–**5f** and **5p** were synthesized in previous literature in our lab [26].

*5.1.2.1. N^1-(3,4-Dimethoxybenzyl)-N^4-(1,2,3,4-tetrahydroacridin-9-yl) butane-1,4-diamine (**5a**).* Intermediate **4a** was reacted with 3, 4-dimethoxybenzaldehyde following the general procedure to give the desired product **5a** as a yellow oil with a yield of 84%. ^{1}H NMR (400 MHz, $CDCl_3$) δ 7.95 (d, J = 7.8 Hz, 1H), 7.90 (d, J = 7.8 Hz, 1H), 7.54 (t, J = 7.0 Hz, 1H), 7.33 (t, J = 7.1 Hz, 1H), 6.88–6.77 (m, 3H), 4.11 (s, 1H), 3.86 (s, 6H), 3.72 (s, 2H), 3.50 (s, 2H), 3.06 (t, J = 5.8 Hz, 2H), 2.73–2.63 (m, 4H), 1.96–1.86 (m, 4H), 1.76–1.68 (m, 2H), 1.66–1.57 (m, 2H). ^{13}C NMR (100 MHz, $CDCl_3$) δ 158.45, 150.71, 148.99, 148.06, 147.43, 132.97, 128.74, 128.29, 123.63, 122.78, 120.25, 120.17, 115.96, 111.37, 111.05, 55.88, 53.86, 49.38, 48.96, 34.04, 29.57, 27.58, 24.90, 23.07, 22.79. Purity: 98.9% by HPLC. HRMS (ESI): calcd for $(M - H)^-$ ($C_{26}H_{36}N_2O_6$) 418.2495, found 418.2497.

*5.1.2.2. N^1-(3,4-Dimethoxybenzyl)-N^5-(1,2,3,4-tetrahydroacridin-9-yl) pentane-1,5-diamine (**5b**).* Intermediate **4b** was reacted with 3, 4-dimethoxybenzaldehyde following the general procedure to give the desired product **5b** as a yellow oil with a yield of 55%. ^{1}H NMR (400 MHz, $CDCl_3$) δ 7.94 (d, J = 8.4 Hz, 1H), 7.90 (d, J = 8.4 Hz, 1H), 7.57–7.49 (m, 1H), 7.37–7.29 (m, 1H), 6.87 (s, 1H), 6.84–6.75 (m, 2H), 3.87 (s, 3H), 3.85 (s, 3H), 3.71 (s, 2H), 3.47 (t, J = 7.2 Hz, 2H), 3.04 (d,

J = 6.1 Hz, 2H), 2.70 (d, J = 5.9 Hz, 2H), 2.62 (t, J = 7.1 Hz, 2H), 2.25 (s, 1H), 1.95–1.85 (m, 4H), 1.72–1.60 (m, 2H), 1.54 (dt, J = 14.1, 6.9 Hz, 2H), 1.48–1.38 (m, 2H). ^{13}C NMR (100 MHz, $CDCl_3$) δ 158.43, 150.70, 148.98, 148.05, 147.43, 132.97, 128.68, 128.24, 123.59, 122.77, 120.23, 120.20, 115.92, 111.46, 111.09, 55.92, 55.86, 53.82, 49.36, 49.15, 33.98, 31.64, 29.77, 24.80, 24.71, 23.03, 22.76. Purity: 98.5% by HPLC. HRMS (ESI): calcd for $(M - H)^-$ ($C_{26}H_{36}N_2O_6$) 432.2651, found 432.2639.

*5.1.2.3. 4–((6-(1,2,3,4-Tetrahydroacridin-9-ylamino)hexylamino)methyl)phenol (**5g**).* Intermediate **4c** was reacted with 4-hydroxy -benzaldehyde following the general procedure to give the desired product **5g** as a yellow oil with a yield of 33%. ^{1}H NMR (400 MHz, $CDCl_3$) δ 7.93 (t, J = 9.1 Hz, 2H), 7.49 (t, J = 7.3 Hz, 1H), 7.30 (t, J = 7.6 Hz, 1H), 7.07 (d, J = 8.4 Hz, 2H), 6.77 (d, J = 8.4 Hz, 2H), 5.98 (s, 1H), 4.09 (s, 1H), 3.66 (s, 2H), 3.47 (t, J = 7.2 Hz, 2H), 3.04 (s, 2H), 2.72–2.51 (m, 4H), 1.86 (d, J = 2.8 Hz, 4H), 1.69–1.56 (m, 2H), 1.57–1.45 (m, 2H), 1.32 (dd, J = 6.3, 3.2 Hz, 4H). ^{13}C NMR (100 MHz, $CDCl_3$) δ 157.98, 157.20, 151.33, 146.64, 129.66, 129.26, 128.70, 127.66, 123.70, 123.01, 119.84, 115.89, 115.30, 53.21, 49.28, 48.72, 33.11, 31.62, 29.30, 26.98, 26.71, 24.71, 22.91, 22.54. Purity: 99.4% by HPLC. HRMS (ESI): calcd for $(M - H)^-$ ($C_{26}H_{36}N_2O_6$) 402.2545, found 402.2529.

*5.1.2.4. 2-Methoxy-4-((6-(1,2,3,4-tetrahydroacridin-9-ylamino)hexyl -amino)methyl)phenol (**5h**).* Intermediate **4c** was reacted with 4-hydroxy-3-methoxybenzaldehyde following the general procedure to give the desired product **5h** as a yellow oil with a yield of 42%. ^{1}H NMR (400 MHz, $CDCl_3$) δ 7.93 (t, J = 7.6 Hz, 2H), 7.51 (t, J = 7.6 Hz, 1H), 7.31 (t, J = 7.8 Hz, 1H), 6.83 (s, 1H), 6.79 (d, J = 8.0 Hz, 1H), 6.70 (dd, J = 8.0, 1.2 Hz, 1H), 4.94 (s, 1H), 3.76 (s, 3H), 3.68 (s, 2H), 3.46 (t, J = 7.2 Hz, 2H), 3.05 (s, 2H), 2.63 (dd, J = 17.2, 9.9 Hz, 4H), 1.88 (s, 4H), 1.69–1.58 (m, 2H), 1.57–1.47 (m, 2H), 1.35 (d, J = 3.1 Hz, 4H). ^{13}C NMR (100 MHz, $CDCl_3$) δ 158.23, 150.97, 147.44, 147.08, 145.66, 130.84, 128.40, 128.30, 123.61, 122.86, 121.00, 120.07, 115.65, 114.87, 111.45, 55.72, 53.77, 49.35, 48.99, 33.58, 31.66, 29.54, 27.06, 26.79, 24.76, 23.00, 22.68. Purity: 97.3% by HPLC. HRMS (ESI): calcd for $(M–H)^-$ ($C_{26}H_{36}N_2O_6$) 432.2651, found 432.2633.

*5.1.2.5. 4-((8-(1,2,3,4-Tetrahydroacridin-9-ylamino)octylamino)methyl) phenol (**5i**).* Intermediate **4e** was reacted with 4-hydroxybenzal -dehyde following the general procedure to give the desired product **5i** as a yellow oil with a yield of 83%. ^{1}H NMR (400 MHz, $CDCl_3$) δ 7.94 (dd, J = 13.4, 8.4 Hz, 2H), 7.49 (t, J = 7.2 Hz, 1H), 7.34–7.28 (m, 1H), 7.08 (d, J = 8.4 Hz, 2H), 6.80 (d, J = 8.4 Hz, 2H), 5.33 (s, 1H), 4.10 (s, 1H), 3.48 (s, 2H), 3.05 (s, 2H), 2.65 (s, 2H), 2.62–2.51 (m, 2H), 1.86 (s, 4H), 1.70–1.55 (m, 2H), 1.48 (s, 2H), 1.24 (dt, J = 14.1, 6.8 Hz, 11H). ^{13}C NMR (100 MHz, $CDCl_3$) δ 158.06, 157.02, 151.30, 146.79, 129.77, 129.56, 128.59, 127.68, 123.60, 123.04, 119.87, 115.82, 115.25, 57.51, 53.32, 49.37, 48.98, 33.15, 31.71, 29.54, 29.31, 29.21, 27.17, 26.79, 24.69, 22.91, 22.55, 18.34. Purity: 99.4% by HPLC. HRMS (ESI): calcd for $(M–H)^-$ ($C_{26}H_{36}N_2O_6$) 430.2818, found 430.2837.

*5.1.2.6. 2-Methoxy-4-((8-(1,2,3,4-tetrahydroacridin-9-ylamino)octylamino)methyl)phenol (**5j**).* Intermediate **4e** was reacted with 4-hydroxybenzaldehyde following the general procedure to give the desired product **5j** as a yellow oil with a yield of 49%. ^{1}H NMR (400 MHz, $CDCl_3$) δ 7.93 (dd, J = 11.5, 8.7 Hz, 2H), 7.51 (t, J = 7.6 Hz, 1H), 7.32 (t, J = 7.6 Hz, 1H), 6.84 (s, 1H), 6.79 (d, J = 8.0 Hz, 1H), 6.70 (d, J = 8.0 Hz, 1H), 4.69 (s, 1H), 3.77 (s, 3H), 3.68 (s, 2H), 3.47 (t, J = 7.1 Hz, 2H), 3.06 (s, 2H), 2.68 (s, 2H), 2.61 (t, J = 7.3 Hz, 2H), 1.88 (s, 4H), 1.62 (dd, J = 14.3, 7.4 Hz, 2H), 1.49 (d, J = 6.3 Hz, 2H), 1.32 (d, J = 29.4 Hz, 8H). ^{13}C NMR (100 MHz, $CDCl_3$) δ 158.31, 150.93, 147.42, 147.23, 145.56, 131.29, 128.44, 128.32, 123.55, 122.87, 120.89, 120.11, 115.64, 114.82, 111.37, 55.71, 53.91, 49.46, 49.28, 33.69, 31.75, 29.77, 29.38, 29.27, 27.24, 26.84, 24.76, 23.02, 22.71. Purity: 99.2% by HPLC. HRMS (ESI): calcd for $(M–H)^-$ ($C_{26}H_{36}N_2O_6$) 460.2964, found 460.2950.

*5.1.2.7. 2,6-Dimethoxy-4-((8-(1,2,3,4-tetrahydroacridin-9-ylamino) octylamino)methyl) phenol (**5k**).* Intermediate **4e** was reacted with 4-hydroxy-3,5-dimethoxybenzaldehyde following the general procedure to give the desired product **5k** as a yellow oil with a yield of 47%. ^{1}H NMR (400 MHz, $CDCl_3$) δ 7.93 (dd, J = 16.5, 8.4 Hz, 2H), 7.54 (t, J = 7.6 Hz, 1H), 7.33 (t, J = 7.5 Hz, 1H), 6.54 (s, 2H), 3.84 (s, 6H), 3.70 (s, 2H), 3.47 (t, J = 7.2 Hz, 2H), 3.06 (s, 2H), 2.70 (s, 2H), 2.62 (t, J = 7.3 Hz, 2H), 1.91 (t, J = 3.2 Hz, 4H), 1.64 (dt, J = 14.6, 7.3 Hz, 2H), 1.50 (dd, J = 13.6, 6.8 Hz, 2H), 1.39–1.24 (m, 8H). ^{13}C NMR (100 MHz, $CDCl_3$) δ 158.37, 150.80, 147.40, 147.21, 133.86, 131.24, 128.68, 128.26, 123.56, 122.83, 120.20, 115.81, 104.89, 56.23, 54.37, 49.50, 49.45, 33.97, 31.75, 29.93, 29.43, 29.30, 27.28, 26.88, 24.78, 23.06, 22.78. Purity: 95.0% by HPLC. HRMS (ESI): calcd for $(M–H)^-$ ($C_{26}H_{36}N_2O_6$) 490.3070, found 490.3046.

*5.1.2.8. 3-((8-(1,2,3,4-Tetrahydroacridin-9-ylamino)octylamino)methyl)phenol (**5l**).* Intermediate **4e** was reacted with 3-hydroxy -benzaldehyde following the general procedure to give the desired product **5l** as a yellow oil with a yield of 44%. ^{1}H NMR (400 MHz, $CDCl_3$) δ 7.84 (dd, J = 11.3, 8.8, 2H), 7.38 (t, J = 7.5, 1H), 7.20 (t, J = 7.6, 1H), 6.99 (t, J = 7.8, 1H), 6.70 (s, 1H), 6.63 (t, J = 7.5, 2H), 5.48 (s, 1H), 3.97 (s, 1H), 3.56 (d, J = 6.7, 2H), 3.38 (dd, J = 12.0, 6.4, 2H), 2.95 (s, 2H), 2.55 (s, 2H), 2.46 (t, J = 7.3, 2H), 1.75 (s, 4H), 1.59–1.43 (m, 2H), 1.41–1.28 (m, 2H), 1.26–1.09 (m, 8H). ^{13}C NMR (100 MHz, $CDCl_3$) δ 158.11, 158.08, 151.31, 146.83, 141.15, 129.49, 128.60, 127.79, 123.62, 123.05, 119.90, 118.90, 115.75, 115.28, 114.69, 53.71, 49.37, 49.02, 33.21, 31.74, 29.61, 29.33, 29.19, 27.14, 26.77, 24.72, 22.94, 22.59. Purity: 98.5% by HPLC. HRMS (ESI): calcd for $(M–H)^-$ ($C_{26}H_{36}N_2O_6$) 430.2858, found 430.2845.

*5.1.2.9. 2-((8-(1,2,3,4-Tetrahydroacridin-9-ylamino)octylamino)methyl)phenol (**5m**).* Intermediate **4e** was reacted with 2-hydroxy -benzaldehyde following the general procedure to give the desired product **5m** as a yellow oil with a yield of 49%. ^{1}H NMR (400 MHz, $CDCl_3$) δ 8.01–7.89 (m, 2H), 7.53 (t, J = 7.5 Hz, 1H), 7.32 (t, J = 7.6 Hz, 1H), 7.13 (t, J = 7.5 Hz, 1H), 6.95 (d, J = 7.2 Hz, 1H), 6.81 (d, J = 7.9 Hz, 1H), 6.75 (t, J = 7.2 Hz, 1H), 5.58 (s, 1H), 4.19 (s, 1H), 3.94 (s, 2H), 3.50 (t, J = 7.1 Hz, 2H), 3.06 (s, 2H), 2.63 (dd, J = 17.6, 10.5 Hz, 4H), 1.88 (s, 4H), 1.73–1.58 (m, 2H), 1.47 (d, J = 6.3 Hz, 2H), 1.42–1.22 (m, 8H). ^{13}C NMR (100 MHz, $CDCl_3$) δ 158.31, 157.72, 151.26, 146.63, 128.63, 128.56, 128.26, 127.82, 123.68, 123.06, 122.66, 119.80, 118.88, 116.25, 115.33, 52.65, 49.35, 48.64, 33.44, 31.65, 29.48, 29.25, 29.19, 26.97, 26.79, 24.69, 22.94, 22.58. Purity: 97.0% by HPLC. HRMS (ESI): calcd for $(M–H)^-$ ($C_{26}H_{36}N_2O_6$) 430.2858, found 430.2841.

*5.1.2.10. N^1-(4-Methoxybenzyl)-N^8-(1,2,3,4-tetrahydroacridin-9-yl) octane-1,8-diamine (**5n**).* Intermediate **4e** was reacted with 4-methoxybenzaldehyde following the general procedure to give the desired product **5n** as a yellow oil with a yield of 96%. ^{1}H NMR (400 MHz, $CDCl_3$) δ 7.92 (dd, J = 14.2, 8.8 Hz, 2H), 7.51 (t, J = 7.6 Hz, 1H), 7.31 (t, J = 7.6 Hz, 1H), 7.20 (d, J = 8.6 Hz, 2H), 6.83 (d, J = 8.7 Hz, 2H), 3.92 (s, 1H), 3.74 (s, 3H), 3.68 (s, 2H), 3.43 (t, J = 7.2 Hz, 2H), 3.04 (d, J = 6.1 Hz, 2H), 2.66 (t, J = 5.4 Hz, 2H), 2.61–2.48 (m, 2H), 1.97–1.76 (m, 4H), 1.70–1.54 (m, 2H), 1.46 (dd, J = 13.6, 6.8 Hz, 2H), 1.36–1.13 (m, 8H). ^{13}C NMR (100 MHz, $CDCl_3$) δ 158.54, 158.38, 150.73, 147.50, 132.53, 129.26, 128.71, 128.17, 123.48, 122.88, 120.22, 115.77, 113.71, 55.19, 53.43, 49.45, 49.31, 34.05, 31.73, 29.98, 29.41, 29.27, 27.23, 26.85, 24.77, 23.05, 22.79. Purity: 98.2% by HPLC. HRMS (ESI): calcd for $(M–H)^-$ ($C_{26}H_{36}N_2O_6$) 444.3015, found 444.2993.

*5.1.2.11. N^1-(Benzo[d] [1,3]dioxol-5-ylmethyl)-N^8-(1,2,3,4-tetrahydroacridin-9-yl)octane-1,8-diamine (**5o**).* Intermediate **4e** was reacted with piperonal following the general procedure to give the desired product **5o** as a yellow oil with a yield of 72%. ^{1}H NMR (400 MHz, $CDCl_3$) δ 7.84 (dd, J = 12.6, 8.6 Hz, 2H), 7.42 (t, J = 7.5 Hz, 1H), 7.22 (t, J = 7.6 Hz, 1H), 6.72 (s, 1H), 6.63 (s, 2H), 5.78 (s, 2H), 4.02 (s, 1H), 3.56 (s, 2H), 3.37 (t, J = 7.2 Hz, 2H), 2.95 (s, 2H), 2.56 (s, 2H), 2.47 (t, J = 7.2 Hz, 2H), 1.78 (s, 4H), 1.53 (dt, J = 14.3, 7.1 Hz, 2H), 1.36 (d, J = 6.2 Hz, 2H), 1.28–1.12 (m, 8H). ^{13}C NMR (100 MHz, $CDCl_3$) δ 157.85, 151.08, 147.62, 146.86, 146.44, 134.13, 128.45, 128.05, 123.58, 122.99, 121.22, 119.89, 115.42, 108.67, 108.00, 100.83, 53.70, 49.36, 49.12, 33.61, 31.66, 29.86, 29.37, 29.24, 27.18, 26.81, 24.70, 22.95, 22.62. Purity: 97.6% by HPLC. HRMS (ESI): calcd for $(M-H)^-$ ($C_{26}H_{36}N_2O_6$) 429.2654, found 429.2636.

*5.1.2.12. N^1-(Pyridin-4-ylmethyl)-N^8-(1,2,3,4-tetrahydroacridin-9-yl) octane-1,8-diamine (**5q**).* Intermediate **4e** was reacted with isonicotinaldehyde following the general procedure to give the desired product **5q** as a yellow oil with a yield of 52%. ^{1}H NMR (400 MHz, $CDCl_3$) δ 8.50 (d, J = 6.0 Hz, 2H), 7.52 (t, J = 7.6 Hz, 1H), 7.34–7.29 (m, 1H), 7.23 (d, J = 5.9 Hz, 2H), 3.76 (s, 2H), 3.47 (t, J = 7.2 Hz, 2H), 3.05 (s, 2H), 2.67 (s, 2H), 2.57 (t, J = 7.2 Hz, 2H), 1.88 (t, J = 3.2 Hz, 4H), 1.71–1.57 (m, 2H), 1.47 (dd, J = 13.7, 6.8 Hz, 2H), 1.40–1.16 (m, 8H). ^{13}C NMR (100 MHz, $CDCl_3$) δ 158.02, 150.94, 149.62, 149.59, 147.02, 128.31, 128.22, 123.51, 122.91, 119.99, 115.53, 52.62, 49.40, 49.33, 33.68, 31.64, 29.93, 29.33, 29.20, 27.09, 26.78, 24.70, 22.95, 22.63. Purity: 99.4% by HPLC. HRMS (ESI): calcd for $(M-H)^-$ ($C_{26}H_{36}N_2O_6$) 415.2862, found 415.2847.

*5.1.3. Synthesis of N-(8-(1,2,3,4-tetrahydroacridin-9-ylamino)octyl) isonicotinamide (**5r**)*

The mixture of pyridine-4-carboxylic acid (86 mg, 0.7 mmol), intermediate **4e** (230 mg, 0.7 mmol), *N,N′*-diisopropylcarbodiimide (100 mg, 0.8 mmol), and 4-dimethylaminopyridine (37 mg, 0.3 mmol) were stirred overnight in CH_2Cl_2 at room temperature. The resulting solution was filtered, and the filtrate was concentrated. The crude product was purified using flash chromatography with chloroform/methanol/ammonia (40:1:0.5%) as elution solvent to give the desired product **5r** as a white solid with a yield of 50% (150 mg), m. p. 90–92 °C, ^{1}H NMR (400 MHz, $CDCl_3$) δ 8.62 (d, J = 6.0 Hz, 2H), 7.96 (d, J = 8.4 Hz, 1H), 7.86 (d, J = 8.4 Hz, 1H), 7.51 (t, J = 7.6 Hz, 1H), 7.32 (s, 1H), 3.85 (s, 1H), 3.47 (t, J = 7.2 Hz, 2H), 3.38 (dd, J = 13.8, 6.6 Hz, 2H), 3.00 (s, 2H), 2.67 (s, 2H), 1.87 (t, J = 3.0 Hz, 4H), 1.71–1.58 (m, 2H), 1.58–1.46 (m, 2H), 1.36–1.22 (m, 8H). ^{13}C NMR (100 MHz, $CDCl_3$) δ 165.64, 158.16, 150.99, 150.20, 147.14, 141.98, 128.36, 128.12, 123.55, 122.97, 121.14, 120.03, 115.57, 49.26, 40.14, 33.68, 31.62, 29.33, 29.03, 26.75, 26.68, 24.70, 22.95, 22.64. Purity: 99.1% by HPLC. HRMS (ESI): calcd for $(M-H)^-$ ($C_{26}H_{36}N_2O_6$) 429.2654, found 429.2641.

5.2. Inhibition studies on AChE and BuChE

Acetylcholinesterase (AChE, E.C. 3.1.1.7, from *electric eel*), butyrylcholinesterase (BuChE, E.C. 3.1.1.8, from *equine serum*), 5,5′-dithiobis-(2-nitrobenzoic acid) (Ellman's reagent, DTNB), butylthiocholine chloride (BTC), acetylthiocholine chloride (ATC), and tacrine hydrochloride were purchased from Sigma Aldrich.

All the assays were carried out in 0.1 M KH_2PO_4/K_2HPO_4 buffer, pH 8.0, using a Shimadzu 2450 Spectrophotometer. Enzyme solutions were prepared at 2.0 units/mL in 2 mL aliquots. The assay medium (1 mL) contained phosphate buffer, pH 8.0, 50 μL of 0.01 M DTNB, 10 μL of enzyme, and 50 μL of 0.01 M substrate (ATC). The assay mixture containing enzyme, buffer, DTNB, and inhibitor was incubated for 15 min, before the substrate was added to start the reaction. The activity was determined by measuring the increase in absorbance at 412 nm in 1 min intervals at 37 °C. The calculations were performed based on the method of Ellman et al. [32]. BuChE assay followed a similar method to that described above.

5.3. Kinetic characterization of AChE inhibition

Kinetic characterization of AChE was carried out following a previously reported method [23]. Six different concentrations of substrate were used, and the assays were carried out in 1 mL 0.1 M KH_2PO_4/K_2HPO_4 buffer, pH 8.0, containing 50 μL of DTNB, 10 μL AChE, and 50 μL substrate. The tested compound was added into the assay solution and pre-incubated with the enzyme at 37 °C for 15 min, followed by the addition of substrate. Kinetic characterization for the hydrolysis of ATC catalyzed by AChE was carried out spectrometrically at 412 nm. The parallel control experiments were carried out without inhibitor in the mixture.

5.4. Measurement of the antioxidation activity

The antioxidation activity was determined by using the oxygen radical absorbance capacity – fluorescein (ORAC-FL) assay [19]. The ORAC-assay measures antioxidant scavenging activity against peroxyl radical induced by 2,2′-azobis(2-amidinopropane) dihydrochloride (AAPH) at 37 °C.

The reaction was carried out in 75 mM phosphate buffer (pH 7.4), and the final reaction mixture was 200 μL. Antioxidant (20 μL) and fluorescein (120 μL, 300 nM final concentration) were placed in the wells of a black 96 well plate, and the mixture was incubated for 15 min at 37 °C. Then AAPH (Aladdin, China) solution (60 μL; 12 mM final concentration) was added rapidly. The plate was immediately placed into a Spectrafluor Plus plate reader (Tecan, Switzerland), and the fluorescence was measured every 60 s for 180 min with excitation at 485 nm and emission at 535 nm. 6-Hydroxy-2,5,7,8-tetramethylchroman-2-carboxylic acid (Trolox, Sigma, Germany) was used as a standard (1–5 μM, final concentration). A blank (FL + AAPH) using phosphate buffer instead of antioxidant and Trolox calibration were carried out in each assay. The samples were measured at different concentrations (1–5 μM), and at least four independent runs were performed for each sample. Fluorescence measurements were normalized based on the curve of the blank (without antioxidant). From the normalized curves, the area under the fluorescence decay curve (AUC) was calculated as:

(1) $AUC = 1 + \sum_{i=1}^{i=90} fi/f0$ Where f_0 is the initial fluorescence at 0 min, and f_i is the fluorescence at time i. The net AUC for a sample was calculated as following:

(2) Net $AUC = AUC_{antioxidant} - AUC_{blank.}$ The ORAC-FL values were calculated as following:

(3) $[(AUC_{Sample} - AUC_{blank})/(AUC_{Trolox} - AUC_{blank})] \times$ [(concentration of Trolox/concentration of sample)], and expressed as Trolox equivalents by using the standard curve calculated for each assay. Final results were in μM of Trolox equivalent/μM of pure compound.

5.5. Molecular modeling

The crystal structure of AChE complexed with tacrine (code ID: 1ACJ) and BuChE complexed with Echothiophate (code ID: 1POI) were obtained in the Protein Data Bank after eliminating the inhibitor and water molecules. The 3D Structure of compound **5j** was built, and its geometry optimization was performed with molecular mechanics. Further preparation of the inhibitor included addition of Gasteiger charges, removal of hydrogen atoms, and addition of their atomic charges to skeleton atoms, and finally, assignment of proper atomic types. Autotors was then used to define the rotatable bonds

in the ligand. Docking studies were carried out using the AUTODOCK 4.0 program. By using ADT, polar hydrogen atoms were added to amino acid residues, and Gasteiger charges were assigned to all atoms of the enzyme. The resulting enzyme structure was used as an input for the AUTOGRID program. AUTOGRID performed a pre-calculated atomic affinity grid maps for each atom type in the ligand, plus an electrostatics map and a separate desolvation map present in the substrate molecule. All maps were calculated with 0.375 Å spacing between grid points. The center of the grid box was placed at the bottom of the active site gorge (AChE [2.781 64.383 67.971]; BuChE [112.0 20.0 40.0]), and the dimensions of the active site box were set at 50 × 46 × 46 Å.

Flexible ligand docking was performed for the compounds. Docking calculations were carried out using the Lamarckian genetic algorithm (LGA), and all parameters were the same for each docking. To ensure the reliability of the results, the docking procedures were repeated independently for 10 times for each compound, and the obtained orientations were analyzed.

5.6. Inhibition of self-mediated Aβ42 aggregation

The thioflavin-T fluorescence method was used. Aβ42 peptide sodium (Anaspec Inc) was dissolved in 0.01 M phosphate buffer (pH 7.4) to obtain a 20 μM solution. Compounds were firstly prepared in DMSO (demethyl sulfoxide) at a concentration of 10 mM. The final concentration of Aβ42 and inhibitors were 20 μM. After incubated in 37 °C for 48 h, thioflavin-T (5 μM in 50 mM glycine–NaOH buffer, pH 8.0) was added. Fluorescence intensity was carried out (excitation at 450 nm and emission at 485 nm). Each measurement was run in triplicate. The fluorescence intensities were recorded, and the percentage of inhibition on aggregation was calculated by using the following equation: $(1 - I_{Fi}/I_{Fc})*100\%$, in which I_{Fi} and I_{Fc} were the fluorescence intensities obtained for absorbance in the presence and absence of inhibitors, respectively, after subtracting the fluorescence of respective blanks.

Conflict of interest

We declare that we have no conflict of interest.

Acknowledgements

We thank the Natural Science Foundation of China (Grants U0832005, 90813011, 30701050), and the Science Foundation of Guangzhou (2009A1-E011-6) for financial support of this study.

Appendix. Supplementary material

Supplementary data related to this article can be found online at doi:10.1016/j.ejmech.2011.03.058.

References

[1] H.F. Kung, C.W. Lee, Z.P. Zhuang, M.P. Kung, C. Hou, K. Plossl, J. Am. Chem. Soc. 123 (2001) 12740–12741.
[2] L.-F. Lau, M.A. Brodney (Eds.), Topics in Medicinal Chemistry: Alzheimer's Disease, vol. 2, Springer, Berlin, 2008, pp. 1–24.
[3] S. Rizzo, C. Riviere, L. Piazzi, A. Bisi, S. Gobbi, M. Bartolini, V. Andrisano, F. Morroni, A. Tarozzi, J.P. Monti, A. Rampa, J. Med. Chem. 51 (2008) 2883–2886.
[4] J.L. Cummings, R. Doody, C. Clark, Neurology 69 (2007) 1622–1634.
[5] A. Cavalli, M.L. Bolognesi, A. Minarini, M. Rosini, V. Tumiatti, M. Recanatini, C. Melchiorre, J. Med. Chem. 51 (2008) 347–372.
[6] M.A. Smith, C.A. Rottkamp, A. Nunomura, A.K. Raina, G. Perry, Biochim. Biophys. Acta 1502 (2000) 139–144.
[7] A. Nunomura, R.J. Castellani, X. Zhu, P.I. Moreira, G. Perry, M.A. Smith, J. Neuropathol. Exp. Neurol. 65 (2006) 631–641.
[8] H.P. Lee, G. Casadesus, X. Zhu, H.G. Lee, G. Perry, M.A. Smith, K. Gustaw-Rothenberg, A. Lerner, Expert Rev. Neurother 9 (2009) 1615–1621.
[9] B.A. Yankner, L.R. Dawes, S. Fisher, L. Villa-Komaroff, M.L. Oster-Granite, R.L. Neve, Science 245 (1989) 417–420.
[10] L.L. Iversen, R.J. Mortishire-Smith, S.J. Pollack, M.S. Shearman, Biochem. J. 311 (Pt 1) (1995) 1–16.
[11] E.D. Thorsett, L.H. Latimer, Curr. Opin. Chem. Biol. 4 (2000) 377–382.
[12] M.S. Wolfe, M. Citron, T.S. Diehl, W. Xia, I.O. Donkor, D.J. Selkoe, J. Med. Chem. 41 (1998) 6–9.
[13] F. Yang, G.P. Lim, A.N. Begum, O.J. Ubeda, M.R. Simmons, S.S. Ambegaokar, P.P. Chen, R. Kayed, C.G. Glabe, S.A. Frautschy, G.M. Cole, J. Biol. Chem. 280 (2005) 5892–5901.
[14] G.P. Lim, T. Chu, F. Yang, W. Beech, S.A. Frautschy, G.M. Cole, J. Neurosci. 21 (2001) 8370–8377.
[15] D.R. Howlett, A.E. Perry, F. Godfrey, J.E. Swatton, K.H. Jennings, C. Spitzfaden, H. Wadsworth, S.J. Wood, R.E. Markwell, Biochem. J. 340 (Pt 1) (1999) 283–289.
[16] M. Ono, M.P. Kung, C. Hou, H.F. Kung, Nucl. Med. Biol. 29 (2002) 633–642.
[17] M. Rosini, E. Simoni, M. Bartolini, A. Cavalli, L. Ceccarini, N. Pascu, D.W. McClymont, A. Tarozzi, M.L. Bolognesi, A. Minarini, V. Tumiatti, V. Andrisano, I.R. Mellor, C. Melchiorre, J. Med. Chem. 51 (2008) 4381–4384.
[18] P. Camps, X. Formosa, C. Galdeano, D. Munoz-Torrero, L. Ramirez, E. Gomez, N. Isambert, R. Lavilla, A. Badia, M.V. Clos, M. Bartolini, F. Mancini, V. Andrisano, M.P. Arce, M.I. Rodriguez-Franco, O. Huertas, T. Dafni, F.J. Luque, J. Med. Chem. 52 (2009) 5365–5369.
[19] L. Fang, B. Kraus, J. Lehmann, J. Heilmann, Y. Zhang, M. Decker, Bioorg. Med. Chem. Lett. 18 (2008) 2905–2909.
[20] M.I. Fernandez-Bachiller, C. Perez, N.E. Campillo, J.A. Paez, G.C. Gonzalez-Munoz, P. Usan, E. Garcia-Palomero, M.G. Lopez, M. Villarroya, A.G. Garcia, A. Martinez, M.I. Rodriguez-Franco, ChemMedChem 4 (2009) 828–841.
[21] H. Tang, F.X. Ning, Y.B. Wei, S.L. Huang, Z.S. Huang, A.S. Chan, L.Q. Gu, Bioorg. Med. Chem. Lett. 17 (2007) 3765–3768.
[22] L. Pan, J.H. Tan, J.Q. Hou, S.L. Huang, L.Q. Gu, Z.S. Huang, Bioorg. Med. Chem. Lett. 18 (2008) 3790–3793.
[23] B. Wang, Y.C. Mai, Y. Li, J.Q. Hou, S.L. Huang, T.M. Ou, J.H. Tan, L.K. An, D. Li, L.Q. Gu, Z.S. Huang, Eur. J. Med. Chem. 45 (2010) 1415–1423.
[24] P.W. Elsinghorst, C.M.G. Tanarro, M. Gutschow, J. Med. Chem. 49 (2006) 7540–7544.
[25] Q. Xie, H. Wang, Z. Xia, M. Lu, W. Zhang, X. Wang, W. Fu, Y. Tang, W. Sheng, W. Li, W. Zhou, X. Zhu, Z. Qiu, H. Chen, J. Med. Chem. 51 (2008) 2027–2036.
[26] W. Luo, Y.P. Li, Y. He, S.L. Huang, J.H. Tan, T.M. Ou, D. Li, L.Q. Gu, Z.S. Huang, Bioorg. Med. Chem. 19 (2011) 763–770.
[27] Y.P. Pang, P. Quiram, T. Jelacic, F. Hong, S. Brimijoin, J. Biol. Chem. 271 (1996) 23646–23649.
[28] A.R. Salomon, K.J. Marcinowski, R.P. Friedland, M.G. Zagorski, Biochemistry 35 (1996) 13568–13578.
[29] W. Linert, M.H. Bridge, M. Huber, K.B. Bjugstad, S. Grossman, G.W. Arendash, Biochim. Biophys. Acta 1454 (1999) 143–152.
[30] P.R. Carlier, Y.F. Han, E.S. Chow, C.P. Li, H. Wang, T.X. Lieu, H.S. Wong, Y.P. Pang, Bioorg. Med. Chem. 7 (1999) 351–357.
[31] J.J. Zhou, H. Huang, S.Q. Xie, Y.X. Wang, J. Zhao, C.J. Wang, Chin. Chem. Lett. 19 (2008) 99–101.
[32] G.L. Ellman, K.D. Courtney, V. Andres Jr., R.M. Feather-Stone, Biochem. Pharmacol. 7 (1961) 88–95.
[33] G.M. Morris, D.S. Goodsell, R.S. Halliday, R. Huey, W.E. Hart, R.K. Belew, A.J. Olson, J. Comput. Chem. 19 (1998) 1639–1662.
[34] W.L. DeLano, The PyMOL Molecular Graphics System. DeLano Scientific, San Carlos, CA, 2002.
[35] M. Bartolini, C. Bertucci, M.L. Bolognesi, A. Cavalli, C. Melchiorre, V. Andrisano, ChemBioChem 8 (2007) 2152–2161.
[36] K. Ono, K. Hasegawa, M. Yamada, H. Naiki, Biol. Psychiatry 52 (2002) 880–886.